

Macroscopic properties of nuclei according to the relativistic mean field theory*

Bożena Nerlo-Pomorska, Katarzyna Mazurek

*Department of Theoretical Physics, Institute of Physics,
Maria Curie-Skłodowska University, 20-031 Lublin, Poland*

Abstract

Self-consistent calculations within the relativistic mean field theory (RMFT) were performed for 150 spherical even-even nuclei. The macroscopic part of the binding energy was evaluated by subtracting the Strutinsky shell corrections from the RMFT energy. The parameters of a liquid-drop (LD), like mass formula which approximates the RMFT results, were determined. The mass and isospin dependence of the RMFT mean-square radii constant for the neutron, proton, charge and total density distributions were estimated. The RMFT liquid-drop parameters and the radii constants are compared with similar results obtained with the Hartree-Fock-Bogoliubov calculations with the Gogny force (HFB+Gogny) and phenomenological models.

PACS numbers: 24.75.+i, 25.85.-w, 25.60.Pj, 25.70-z

1 Introduction

Self-consistent Hartree-Fock (HF) calculations with effective nucleon-nucleon forces of the Gogny [1] and Skyrme [2] type, or within the relativistic mean field theory (RMFT) [3] are nowadays able to describe many features of nuclei. The theoretical results agree with the experimental data and the

*The work was partially sponsored by the State Committee for Scientific Research under contract No. 2 P03B 115 19 and the collaboration between IN2P3 and Polish laboratories nr 99-95

masses, charge and neutron radii, electric multipole moments or energies of the lowest excited states are well reproduced even for nuclei beyond the stability line. It is probable that the presently accessible nuclei with the large neutron excess demand some revision of the parameters used in the traditional models, which have been adjusted to the smaller amount of data around the β stable nuclei.

It is also interesting to compare the self-consistent prescriptions with other simpler models and see how they work for the nuclei close to the proton or neutron drip lines. The macroscopic-microscopic method with the liquid-drop (or droplet) model, using the Strutinsky shell correction and various kinds of the single-particle average potentials is of special interest because of its simplicity. Is it possible to extract the shell effects from the self-consistent energy and obtain an estimate of the macroscopic energy hidden in these models? This was already done successfully for the Skyrme [4] and Gogny [5] forces and now we would like to apply a similar method for the relativistic mean field (RMF). Nevertheless, one has to remember that the weak binding effects at drip lines are of purely quantal origin and the application of macroscopic-microscopic method could be questionable there.

In Section II a short overview of the RMFT equations and parameters is given and the prescription for shell correction [6] is recalled. Moreover the liquid-drop formulae for the macroscopic energy and the root mean square (r.m.s.) radii of the proton, neutron and charge distributions are mentioned. In Section III the macroscopic part of the RMFT energy is approximated by a liquid-drop like formula. The liquid-drop parameters corresponding to the macroscopic part of the RMFT binding energy are compared with those of other theoretical and phenomenological models. In Section IV the RMFT root mean-square radii of 150 even-even spherical nuclei are approximated by the isospin-dependent formulae and compared with other experimental and theoretical estimates. The ratio of proton to neutron radius is of special interest due to the lack of experimental data for neutron radii. One can use this ratio to predict the neutron r.m.s. radius of a nucleus when its charge radius is known. At the end of the paper the conclusions are drawn and further investigations proposed.

2 Theory

The single-particle level scheme obtained within the self-consistent RMFT calculation is used to evaluate the shell correction (E_{shell}) to the binding energy:

$$E_{\text{shell}} = \sum_{\text{occ}} 2e_{\nu} - \tilde{E} , \quad (1)$$

where the sum runs over all occupied levels. All the single-particle levels up to the cut-off energy lying 15 MeV above the Fermi surface, are used to obtain the smoothed energy from the Strutinsky integral. We haven't apply the newer prescription for the shell correction proposed in Ref. [7] to avoid the single-particle continuum effect because we wished to compare our results with those of reference [5] obtained with the classical Strutinsky prescription. Nevertheless, the single-particle levels scheme for each nucleus, especially for the neutron-rich ones was carefully checked in order to take into account the proper number of single-particle states around Fermi surface. It was not our aim to estimate the position of the drip lines, but to obtain the average dependence of binding energy on A, Z number. For the detailed calculation of the binding energies of the nuclei close to the proton or neutron drip lines the use of the prescription of Ref. [7, 8] would be necessary. The Strutinsky smooth energy \tilde{E} is equal to

$$\tilde{E} = 2 \int_{-\infty}^{\lambda} e \bar{\rho}(e) de . \quad (2)$$

The average levels density $\bar{\rho}(e)$ was obtained by the smoothing of the single-particle levels density $\rho(e) = \sum_{\nu} \delta(e - e_{\nu})$ with the Gauss function multiplied by the 6th order correction polynomial f

$$\bar{\rho}(e) = \frac{1}{\gamma \sqrt{\pi}} \int_{-\infty}^{+\infty} \rho(e') e^{-\left(\frac{e-e'}{\gamma}\right)^2} f\left(\frac{e-e'}{\gamma}\right) de' . \quad (3)$$

The width parameter of the Gauss function $\gamma = 1.2\hbar\omega$, with $\hbar\omega = 40A^{-1/3}$ MeV, corresponds to the average position of the Strutinsky plateau in the shell corrections for the chosen sample of 150 spherical even-even nuclei. The average single-particle levels density obtained with the RMFT is close to the results obtained in Ref. [5] for the Gogny force.

The macroscopic part of the binding energy is equal to the difference between the self-consistently calculated RMFT energy (E_{RMFT}) without pairing

interaction and the total (neutron and proton) shell correction

$$E_{\text{macr}}^{\text{RMFT}} = E_{\text{RMFT}} - E_{\text{shell}}^n - E_{\text{shell}}^p . \quad (4)$$

These quantities, evaluated for several nuclei with mass numbers A and isospins $I = (N - Z)/A$ are approximated by the liquid-drop formula of Myers-Świątecki type [9]

$$E_{\text{macr}} = -b_{\text{vol}}(1 - \kappa_{\text{vol}} I^2)A + b_{\text{surf}}(1 - \kappa_{\text{surf}} I^2)A^{2/3} + b_{\text{Coul}}Z^2 A^{-1/3} - C_4 Z^2/A \quad (5)$$

where b_{Coul} is connected with the charge radius parameter r_0^{ch} by $b_{\text{Coul}} = \frac{3}{5}e^2/r_0^{\text{ch}}$.

The nucleon densities $\rho_n(\vec{r})$ and $\rho_p(\vec{r})$ obtained within the RMFT + BCS model could be used to evaluate the mean-square radii of the neutron or proton distributions. Here the question of the validity of that approach for the nuclei near drip line rises again, but the influence of pairing forces on the nuclear radius calculated in various models (HFB + Gogny, LD + Woods Saxon) is similar and does not interfere with the isotopic shifts, which have been measured

$$\langle r^2 \rangle_q = \int \rho_q(\vec{r}) \vec{r}^2 dV / \int \rho_q(\vec{r}) dV , \quad q = \{n, p\} . \quad (6)$$

Knowing the mean square radius $\langle r^2 \rangle$ one can define an equivalent spherical sharp radius R using the following relation $\langle r^2 \rangle = \frac{3}{5}R^2$, which arises directly from Eq. (6) for the uniform density distribution $\rho_q = \frac{\mathcal{N}_q}{4/3\pi R^3}$, with $\mathcal{N}_q = \{N, Z\}$ and the volume conservation condition. In a rough estimate one usually assumes that $R = r_0 A^{1/3}$, and takes the radius constant $r_0 = 1.2$ fm. However this formula turns out to be too approximate and it was proved in Ref. [10] that a similar formula but using an isospin dependent radius constant, described the experimental data in a more satisfactory way. We have shown that the measured or calculated mean-square radii within the RMFT [11] or HFB+Gogny [5] models could be accurately reproduced when the radius constant has the following form

$$r_0 = r_{00}(1 + \alpha I + \kappa/A) , \quad (7)$$

where r_{00} , α , and κ are free adjustable parameters. The ratio of the proton to neutron root mean-square radii could be described by a formula similar to the one given above and could be used to predict the radius of the neutron

distribution when the charge radius is measured [11, 5]. One has to note that this ratio does not depend on deformation in a first approximation since the density distributions of neutrons and protons are close to each other also for deformed nuclei.

3 Binding energies

The RMFT calculations with the NL3 set of parameters were performed for 150 even-even nuclei between the proton and neutron drip lines which have, according to Ref. [12] a quadrupole moment almost equal to zero. They are: $^{38-50}\text{Ca}$, $^{82-90}\text{Sr}$, $^{96-140}\text{Sn}$, $^{80-84}\text{Sm}$, $^{162-220}\text{Pb}$ isotopes, $N = 50$ with $A \in (86, 92)$, $N = 82$ with $A \in (122, 164)$, and $N = 126$ with $A \in (174, 224)$ isotones and 30 other spherical nuclei along the β stability line. This choice of nuclei had already been used to estimate the shell effects by the HF method with the Gogny force [5]. This set of representative spherical nuclei is larger than the sample of 30 deformed nuclei taken for the radii calculation within the RMFT in Ref. [11].

We have used $N_0 = 20$ shells and the oscillator length constant $b = 2.4$ MeV of the harmonic oscillator as the basis when solving the self-consistent RMFT equations for fermions. At first the calculations were performed without taking into account the pairing residual interaction in order to evaluate the Strutinsky shell corrections, and then the experimental proton and neutron pairing energy gaps Δ_p , Δ_n were used to evaluate the r.m.s. radii and the potential energies in the RMFT + BCS model. This simplified way of pairing correlation inclusion does not influence the values of radii significantly even for the nuclei near the drip lines.

3.1 Liquid-drop parameters

Fig. 1 shows the RMFT (solid lines) shell corrections in comparison with the results of Ref. [5] (dashed lines) obtained for the Gogny force. In the first panel of the multiplot one can observe the dependence on A of the total shell correction $E_{\text{shell}}^{\text{tot}}$ for six groups of Ca-Th isotopes, in the middle $E_{\text{shell}}^{\text{tot}}$ for three groups of $N = 50, 82, 126$ isotones and in the r.h.s. panel for β stable isotopes.

The shell corrections obtained in both theoretical models are similar. They exhibit minima for the same magic numbers of one kind of nucleons and

differ from each other by no more than a few MeV. The RMFT estimates of the macroscopic part of the binding energy obtained by subtracting the total shell correction from the self-consistent RMFT energy (Eq. 4) for the above set of nuclei were fitted by the liquid-drop formula (5), and the following set of parameters was obtained

$$\frac{E_{\text{macr}}^{\text{RMFT}}}{\text{MeV}} = -15.19(1 - 1.66I^2)A + 16.81(1 - 1.21I^2)A^{2/3} + 0.68\frac{Z^2}{A^{1/3}} - 1.3\frac{Z^2}{A} . \quad (8)$$

The r.m.s. deviation of the fit was equal to 1.97 MeV. In the Table I these RMFT estimates of the LD parameters are compared with the traditional (MS-1967) Myers-Świątecki liquid-drop formula [9]. What is more Table I shows the modern phenomenological set (MS-2002) [13] fitted to presently available experimental masses [14] when using the microscopic (shell+pairing+deformation) energy corrections from Ref. [12]. In the last column of Table I are given the results obtained in [5] within the Hartree-Fock calculation with the Gogny D1S force [1] which turned out to be similar to these of RMFT.

During the last 35 years, as seen in Table I, the liquid-drop parameters reproducing the experimental data have not changed very much. The macroscopic part of the binding energies obtained with the Gogny force [5] is described by the set of the LD parameters which approximates to the newest fit (MS-2002) of the LD parameters adjusted to the presently known experimental masses [14]. The results obtained within the RMFT give smaller values of the volume and surface energies, while the charge radius constant corresponding to the Coulomb energy is equal to 1.264 fm and is substantially larger than its present phenomenological value (1.191 fm). By contrast, the RMFT estimate of the C_4 parameter, which is responsible for the charge diffuseness effect, is much closer to its phenomenological value compared with the Gogny's one. The volume and surface dependence on isospin is weaker in the RMFT than the experimental one. The Gogny force gives a slightly stronger dependence of both energies than the phenomenological (MS-2002) one.

We can compare the three models in Fig. 2. The results of MS-2002 liquid-drop model and Gogny are subtracted from the macroscopic energies of the RMFT and shown for all the groups of nuclei in dependence on A . Since the RMFT macroscopic energy (solid lines) is the smallest, it gives the largest binding. The Gogny results are closer to the RMFT ones than to the

phenomenological (MS-2002) binding energy.

The differences between the binding energies obtained with these three models reach even -30 MeV for isotope and isotone chains while for β stable isotopes they stay within -20 MeV. This is understandable because the NL3 set of parameters of the RMFT was fitted for nuclei close to the β stability line. The binding energies obtained with the Gogny force are closer to the liquid-drop estimates than these of RMFT. The isospin dependence of the binding energies is not well reproduced by either of the both models.

4 Mean-square radii

It is a known fact that the pairing correlations influence the density distribution in nuclei. Therefore in order to evaluate the neutron and proton mean-square radii within the RMFT, we have to include the pairing forces. This was done in a simplified way by inserting into the BCS equations the experimental proton and neutron energy gap between the ground state and the first excited two-quasiparticle state of even-even nuclei. The pairing energy gaps are extracted from the experimental binding energies [15] with the help of a three parameter formula proposed in Ref. [17]

$$\Delta_q = \frac{\pi \mathcal{N}_q}{2} [(B(\mathcal{N}_q - 1) - 2B(\mathcal{N}_q) + B(\mathcal{N}_q + 1))] , \quad q = \{n, p\} , \quad (9)$$

where $\pi_{\mathcal{N}_q} = (-1)^{\mathcal{N}_q}$ and \mathcal{N}_q denotes nucleon number N for neutrons, Z for protons. When the BCS equations are solved the pairing correlations are added to the self-consistent mean field.

The resulting r.m.s. radii for neutron and charge distributions as well as the ratio of proton to neutron radii are plotted in Figs. 3 - 5 for the three groups of isotopes, isotones and β stable nuclei. The RMFT radii can be easily reproduced by the isospin dependent formula (7), which corresponds to the sharp density distribution. The RMFT radius constants fitted for the 150 spherical nuclei are:

for neutrons

$$r_0^n = 1.17(1 + 0.27I + 3.38/A) \text{ fm} , \quad (10)$$

for protons

$$r_0^p = 1.22(1 - 0.15I + 1.51/A) \text{ fm} , \quad (11)$$

and for charge distribution

$$r_0^{\text{ch}} = 1.23(1 - 0.15I + 2.47/A) \text{ fm} . \quad (12)$$

The r.m.s. deviation of each fit was smaller than 0.01 fm. The estimates (10-12) are very close to those obtained in Ref. [11] for the smaller sample (30) of deformed nuclei. This means that the deformation dependent function renormalizing the distributions to the sphere was properly chosen in Ref. [11], and that the formulae (10-12) adequately describe the radii constants, not only for the spherical but also for the deformed nuclei.

This is also the case with the proton to neutron ratio

$$\frac{r_p}{r_n} = 1.04(1 - 0.38I - 1.52/A), \quad (13)$$

which can be used to estimate the neutron radii with the help of the measured charge radius

$$r_n = \frac{\sqrt{r_{\text{ch}}^2 - 0.64\text{fm}^2}}{1.04(1 - 0.38I - 1.52/A)} \quad (14)$$

producing good agreement (with a slight tendency to overestimate) with the 14 experimentally known neutron radii of Ref. [18]. In contrast, a similar ratio obtained with the Gogny force in [5] gives a slightly smaller neutron radius. Both groups of neutron radii for the 14 experimentally known data can be seen in Fig. 3 in dependence on the reduced isospin I .

In Fig. 4 the differences between the charge radii predicted by the RMFT and the Gogny model (solid lines) are compared with the experimental data [18] from which also the Gogny radii are subtracted (crosses). One can see that the agreement of the RMFT results for the charge radii with the experimental data is even slightly better than that of Ref. [5] obtained with the Gogny force.

In Fig. 5 the proton to neutron radius ratio obtained in the RMFT (solid lines) and with the Gogny force (dashed lines) is compared with the experimental data (crosses) [18, 19] for the three groups of isotopes, isotones and β stable nuclei.

The parameters of formulae (10-12) obtained for various theoretical models are compared in Table II with the ones fitted to the experimental data [18, 19] and in Ref. [10] for charge radii.

Both self-consistent theoretical models give similar estimates of the r_{00} parameter of neutron, proton, and charge radii. The isospin dependence of the r.m.s. radii is slightly different in the two models. The κ/A term, important for the light nuclei, shows some differences as well.

5 Conclusions

The following conclusions can be drawn from our investigation:

1. The shell corrections obtained in the RMFT with the NL3 set of parameters and within the Hartree-Fock mean field calculation with the Gogny D1S force are similar.
2. The volume and surface parts of the binding energy in the RMFT are smaller than the corresponding energies obtained with the Gogny model [5] as well as than those of the liquid-drop model fitted to the experimental masses [9, 13].
3. The isospin dependence of the volume and surface term obtained within the RMFT is too small in comparison with the phenomenological liquid-drop model.
4. The mean-square radii of the proton, neutron and charge distributions are similar in the Gogny and RMFT models.
5. The RMFT ratio of proton to neutron radii, used to predict the neutron radii when the charge radius is known, gives the estimates within experimental error bars for all 14 experimentally known neutron radii.

Similar effects for deformed nuclei with various sets of RMFT parameters will be investigated soon.

Acknowledgments

We would like to thank professors Klaus Dietrich and Peter Ring for fruitful discussions and the warm hospitality during our stay at the Technische Universität München. The help of Krzysztof Pomorski in formulating the manuscript is also appreciated.

References

- [1] J. F. Berger, M. Girod and D. Gogny, Comput. Phys. Commun. **63**, 365 (1991).
- [2] E. Chabanat, P. Bonche, P. Haensel, J. Mayer and R. Schaefer, Nucl. Phys. **A635**, 231 (1998).
- [3] G.A. Lalazissis, J. König, P. Ring, Phys. Rev. **C55**, 540 (1996).
- [4] M. Brack, R. K. Bhaduri, Semiclassical Physics, Addison-Wesley Publ. Comp. (1998).
- [5] M. Kleban, B. Nerlo-Pomorska, J. F. Berger, J. Dechargeé, M. Girod and S. Hilaire, Phys. Rev. **C65**, 024309 (2002).
- [6] V. M. Strutinsky, Nucl. Phys. **A95**, 420 (1967).
- [7] A. T. Kruppa, Phys. Lett. **B431**, 237 (1998).
- [8] T. Vertse, A. T. Kruppa and W. Nazarewicz, Phys. Rev **C61**, 064317 (2000).
- [9] W. D. Myers, W. J. Świątecki, Nucl. Phys. **81**, 1 (1966); Ark. Phys. **36**, 343 (1967).
- [10] B. Nerlo-Pomorska, K. Pomorski, Z. Phys. **A348**, 169 (1994).
- [11] M. Warda, B. Nerlo-Pomorska, and K. Pomorski, Nucl. Phys. **A635**, 484 (1998).
- [12] P. Möller, J. R. Nix, W. D. Myers, W. J. Świątecki, At. Data Nucl. Data Tables **59** (1995) 185.
- [13] K. Pomorski and J. Dudek, preprint in nucl-th/0205011
- [14] M.S. Antony, Nuclide Chart 2002, Strasbourg, France, Association Européenne contre les Leucodistrophies.
- [15] G. Audi and A. H. Wapstra, Nucl. Phys. **A565**, 1 (1993).
- [16] W.D. Myers and W.J. Świątecki, Nucl. Phys. **A601**, 141 (1996).

- [17] W. Satuła, J. Dobaczewski and W. Nazarewicz, Phys. Rev. Lett. **81**, 3599 (1998).
- [18] G. Fricke, C. Bernardt, K. Heiling, L. A. Schaller, L. S. Schellenberg, E. B. Shera and C. W. de Jager, At. Data Nucl. Data Tables **60**, 177 (1995).
- [19] C. J. Batty, E. Friedman, H. J. Gils and H. Rebel, Adv. Nucl. Phys. **19**, 1 (1989).

Table 1: The macroscopic energy parameters.

| parameter | unit | MS-1967 | MS-2002 | RMFT | Gogny |
|------------------------|------|---------|---------|--------|--------|
| b_{vol} | MeV | 15.667 | 15.848 | 15.185 | 15.649 |
| κ_{vol} | – | 1.790 | 1.848 | 1.657 | 1.916 |
| b_{surf} | MeV | 18.560 | 19.386 | 16.811 | 18.928 |
| κ_{surf} | – | 1.790 | 1.983 | 1.209 | 2.108 |
| r_0^{ch} | fm | 1.205 | 1.190 | 1.264 | 1.188 |
| C_4 | MeV | 1.211 | 1.200 | 1.299 | 2.015 |

Table 2: The radii parameters.

| | Phen. | Gogny (150 sph.n.) | RMFT (30 def.n) | RMFT (150 sph.n.) |
|-----------------|--------------|--------------------|-----------------|-------------------|
| <u>neutrons</u> | [19] | [5] | [11] | |
| r_{00} | 1.17 | 1.17 | 1.17 | 1.17 |
| α | 0.16 | 0.12 | 0.25 | 0.27 |
| κ | 3.85 | 3.29 | 2.81 | 3.38 |
| <u>protons</u> | [18] | | | |
| r_{00} | 1.22 | 1.21 | 1.24 | 1.22 |
| α | -0.17 | -0.14 | -0.16 | -0.15 |
| κ | 1.78 | 1.83 | 0.65 | 1.51 |
| <u>charge</u> | [18]([10]) | | | |
| r_{00} | 1.24(1.25) | 1.22 | 1.24 | 1.23 |
| α | -0.19(-0.25) | -0.15 | -0.15 | -0.15 |
| κ | 1.65(2.06) | 2.32 | 0.58 | 2.47 |
| <u>ratio</u> | [18, 19] | | | |
| r_{00} | 1.03 | 1.04 | 1.05 | 1.04 |
| α | -0.36 | -0.27 | -0.36 | -0.38 |
| κ | -1.33 | -1.12 | -3.15 | -1.52 |

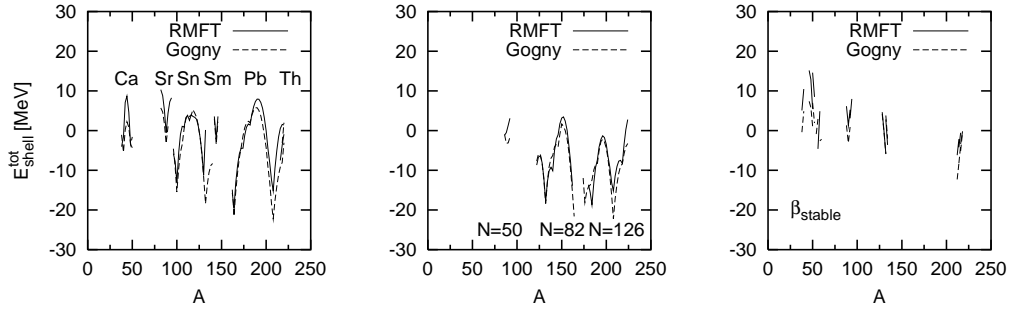


Figure 1: The total shell corrections obtained within the RMFT (solid lines) and with the Gogny force (dashed lines) in dependence on the mass number A . The three parts of multiplot show the shell corrections of Ca-Th isotopes, for the $N = 50, 82, 126$ isotones and for the β stable nuclei respectively.

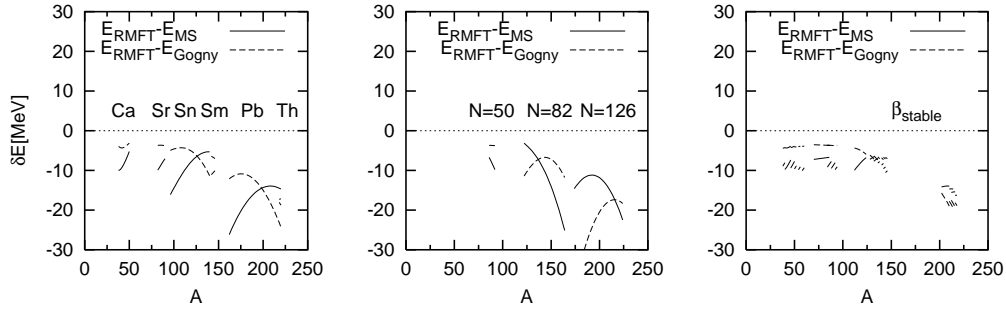


Figure 2: The comparison of macroscopic energies obtained within the RMFT and with the Gogny [5] force and the liquid-drop energies [13] in dependence on A . The differences between the RMFT macroscopic parts of the binding energies (solid lines) and the phenomenological (MS-2002) [13] (solid lines) estimates are compared with the corresponding differences between RMFT and the Gogny [5] macroscopic energies (dashed lines) for the isotopes (l.h.s.) isotones (middle) and β stable nuclei (r.h.s.).

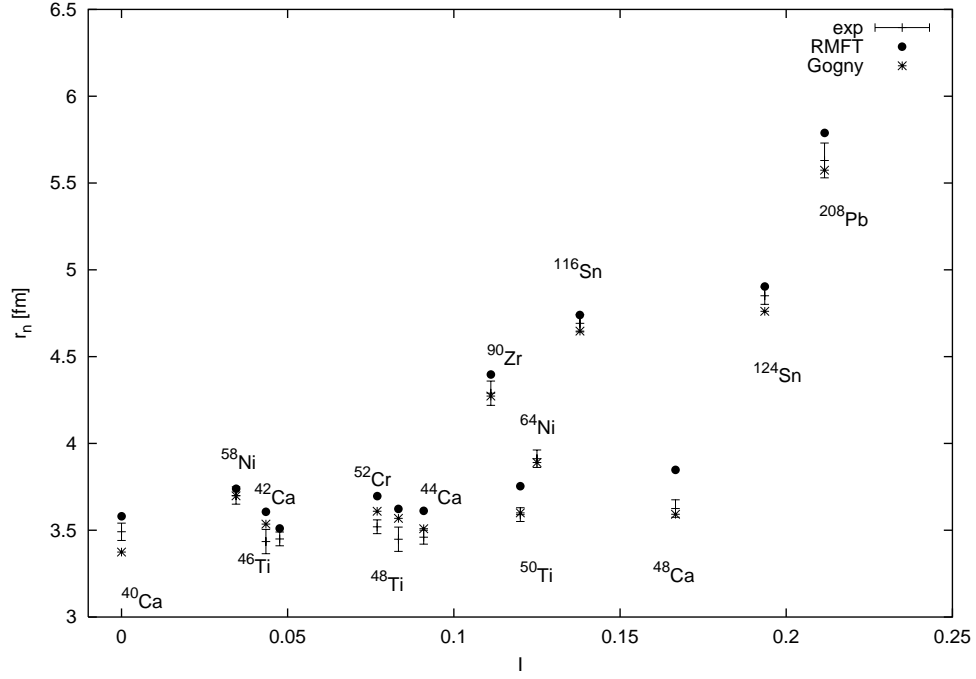


Figure 3: The 14 experimentally known neutron radii from Ref. [19] (crosses) are compared with the RMFT predictions (spheres) and the estimates done with the Gogny model (stars) in dependence on the reduced isospin $I = (N - Z/A)$.

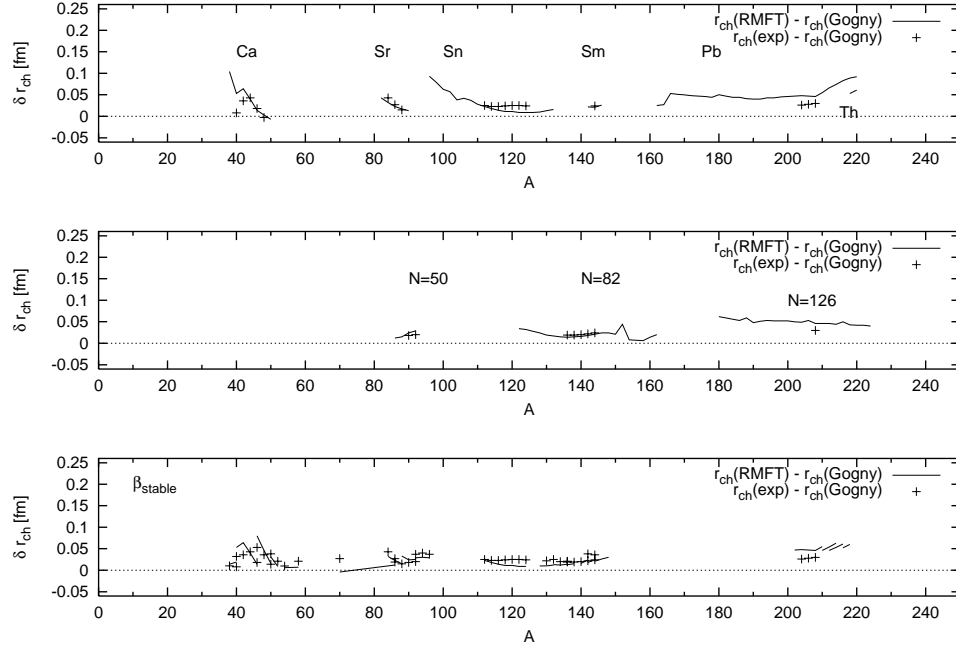


Figure 4: The charge radii predicted by the RMFT related to the results of the Gogny model (solid lines) are compared with the experimental data [18] from which the same reference of Gogny charge radii is also removed (crosses). The three panels correspond to the isotopes (up) isotones (middle) and β stable nuclei (down).

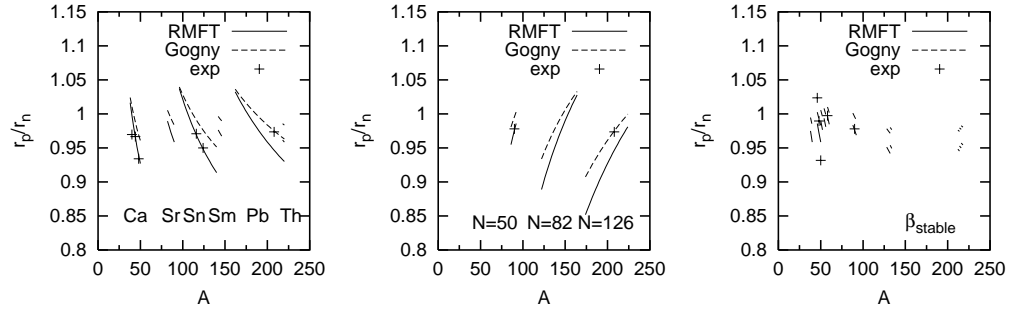


Figure 5: The proton to neutron radius ratio obtained in the RMFT (solid line) and with the Gogny force (dashed lines) is compared with the similar ratio obtained on the basis of the experimental data (crosses) [18, 19]. The three parts of multiplot show the calculated root mean-square radii ratios for the three groups of isotopes (l.h.s.), isotones (middle) and β stable nuclei (r.h.s.) [5].